Çukurova Üniversitesi
Mühendislik Fakültesi Dergisi
Çukurova University
Journal of the Faculty of Engineering
ISSN: 2757-9255 CİLT/VOLUME: 41 SAYI/ISSUE: 2 HAZİRAN/JUNE 2026

Numerical Investigation of Channel Configuration on Thermal Behavior of Liquid-Cooled Plates in Cylindrical Lithium-Ion Battery Modules

Sinan KEYİNCİ [1,a]

[1]*Çukurova University, Faculty of Engineering, Department of Automotive Engineering, Adana, Türkiye*

[a]***ORCID***: *0000-0003-2948-3846*

Article Info
Received : 07.11.2025
Accepted : 06.01.2026
DOI: 10.21605/cukurovaumfd.1819609
Corresponding Author
Sinan KEYİNCİ
skeiyinci@cu.edu.tr
Keywords
Liquid cooling plate
Electric vehicles
Lithium-ion battery
Battery thermal management
Computational fluid dynamics

How to cite: *KEYİNCİ, S., (2026). Numerical Investigation of Channel Configuration on Thermal Behavior of Liquid-Cooled Plates in Cylindrical Lithium-Ion Battery Modules. Cukurova University, Journal of the Faculty of Engineering, 41(2), 271-283.*

ABSTRACT

This study numerically investigates liquid cooling plates (LCPs) for cylindrical 18650 lithium-ion battery packs under varying channel geometries and inlet velocities. Three-dimensional transient CFD simulations were conducted to analyze the coupled thermal and fluid behavior. Two coolants, water and a 50:50 (v:v) water-ethylene glycol mixture, were tested at inlet velocities of 0.1, 0.25, and 0.5 m/s. Results show that the configuration with fewer, wider channels achieved the lowest maximum temperature ($T_{max} \approx 305$ K) and the most uniform temperature field ($\Delta T < 3$ K). Increasing the number of channels reduced channel height and local convection, leading to higher gradients and non-uniform flow near the outlet. Increasing velocity from 0.1 to 0.25 m/s improved cooling performance by about 40%, while a further increase had an insignificant effect (<1 K). As a result of this study, a moderate flow rate combined with an optimized channel geometry provided the best balance between heat dissipation and flow uniformity for compact electric vehicle battery modules.

Silindirik Lityum-İyon Pil Modüllerindeki Sıvı Soğutmalı Plakaların Termal Davranışında Kanal Yapılandırmasının Sayısal İncelenmesi

Makale Bilgileri
Geliş : 07.11.2025
Kabul : 06.01.2026
DOI: 10.21605/cukurovaumfd.1819609
Sorumlu Yazar
Sinan KEYİNCİ
skeiyinci@cu.edu.tr
Anahtar Kelimeler
Sıvı soğutma plakası
Elektrikli araçlar
Lityum-iyon batarya
Batarya termal yönetimi
Hesaplamalı akışkanlar dinamiği

Atıf şekli: *KEYİNCİ, S., (2026). Silindirik Lityum-İyon Pil Modüllerindeki Sıvı Soğutmalı Plakaların Termal Davranışında Kanal Yapılandırmasının Sayısal İncelenmesi. Çukurova Üniversitesi, Mühendislik Fakültesi Dergisi, 41(2), 271-283.*

ÖZ

Bu çalışma, silindirik 18650 tipi lityum-iyon batarya paketleri için farklı kanal geometrileri ve giriş hızları altında sıvı soğutma plakalarını sayısal olarak incelemektedir. Üç boyutlu zamana bağlı CFD simülasyonları kullanılarak ısıl ve akışkan davranışının etkileşimi analiz edilmiştir. Soğutucu akışkan olarak saf su ve hacimce 50:50 oranında karıştırılmış su-etilen glikol karışımı kullanılmış; giriş hızları 0.1, 0.25 ve 0.5 m/s olarak belirlenmiştir. Sonuçlar, daha az sayıda ve daha geniş kanallara sahip konfigürasyonun en düşük maksimum sıcaklığı ($T_{max} \approx 305$ K) ve en homojen sıcaklık dağılımını ($\Delta T<3$ K) sağladığını göstermektedir. Kanal sayısının artırılması, kanal yüksekliğini ve yerel taşınımı azaltarak çıkış bölgesinde daha yüksek sıcaklık gradyenlerine ve akış düzensizliklerine yol açmıştır. Akış hızının 0,1 m/s'den 0,25 m/s'ye çıkarılmasıyla soğutma performansı yaklaşık %40 oranında artmış, ancak daha yüksek hızlarda bu artış ihmal edilebilir düzeyde kalmıştır (<1 K). Çalışma sonucunda, orta düzeyde bir akış hızı ile optimize edilmiş kanal geometrisinin, kompakt elektrikli araç batarya modülleri için ısı dağılımı ve akış homojenliği arasında en uygun dengeyi sağlamıştır.

1. INTRODUCTION

The transportation industry has been undergoing a profound transformation toward electrification, driven by the urgent need to reduce greenhouse gas emissions and mitigate dependence on fossil fuels [1-3]. According to the latest climate assessments, road transportation is responsible for approximately 15% of global CO_2 emissions, highlighting the critical role of widespread electric vehicle (EV) adoption in achieving climate goals [4]. EV production has accelerated significantly, supported by government incentives and rapid developments in energy storage technologies.

Among the available energy storage solutions for EVs, lithium-ion batteries (LiBs) have emerged as the preferred choice due to their high energy density, low self-discharge rate, and long cycle life [5,6]. Nevertheless, the thermal sensitivity of LiBs remains a major limitation affecting both performance and safety. Elevated operating temperatures accelerate side reactions and active material degradation, while subzero conditions impede ion transport and increase internal resistance, leading to reduced capacity and power losses [7]. For optimal operation, the temperature of each cell should be maintained within approximately 15-35 °C, and the temperature deviation between cells (ΔT) should not exceed 5 °C to ensure uniform aging and safe operation [8-10]. To achieve these conditions, an efficient battery thermal management system (BTMS) is indispensable.

Existing BTMS approaches can be broadly classified into air-cooled, liquid-cooled, phase change material-based, and heat pipe-assisted systems [11]. Among existing approaches, liquid cooling has become the dominant choice for high-power-density battery modules due to its superior heat dissipation, space efficiency, and accommodating complex module geometries [12]. Within this category, liquid cooling plates (LCPs), featuring internal channels that circulate coolant beneath or between the cells, have become the preferred solution in modern EV packs. The effectiveness of an LCP depends strongly on the geometry of its cooling channels, such as the number, height, and layout pattern [13]. Non-uniform flow distribution can lead to hot spots and accelerated degradation, whereas overly large channels increase system mass and pumping losses.

Extensive efforts have been made to enhance the cooling efficiency and temperature uniformity of LCPs through channel geometry optimization. For instance, Li et al. [14] explored Tesla-type mini-channel structures and applied genetic algorithms to optimize key geometric parameters. Their results showed that specific combinations of channel width and spacing significantly reduced thermal resistance while maintaining low pressure drop. These findings highlight the strong link between geometric scale and flow smoothness, demonstrating that small size adjustments can provide significant thermal benefits. Similarly, Lai et al. [15] developed an LCP incorporating grooves and secondary microchannels, enhancing surface contact and coolant mixing. Their simulation results confirmed better heat extraction and reduced hotspot formation compared to conventional flat channel designs. Akbarzadeh et al. [16] compared air-cooled and U-shaped LCP systems, finding that the U-type LCP design significantly improved thermal uniformity in high-energy battery modules. Dubey et al. [17] evaluated serpentine and U-shaped microtextured cooling channels for LiB modules and demonstrated that serpentine paths not only offered lower thermal resistance but also achieved enhanced temperature uniformity due to extended surface area and longer coolant residence time. Their simulations and experimental results indicated that the micro-texturing of channel walls further intensified convective heat transfer, particularly in the serpentine configuration, by promoting turbulent flow and improving local Nusselt numbers. It can be inferred that both the macro-scale arrangement of flow channels and the micro-scale surface features contribute synergistically to improving overall heat-transfer performance. Finally, Monika et al. [18] performed a multi-objective optimization of a hexagonal mini-channel LCP for LiB modules, focusing on minimizing maximum cell temperature, reducing pressure drop, and enhancing heat transfer. The best design achieved a 62.3% reduction in pressure drop and 64.4% improvement in heat transfer coefficient without significant thermal penalty, demonstrating that nonconventional geometries, such as hexagonal layouts, can offer a well-balanced thermal performance for compact EV applications.

While these studies have considerably advanced the understanding of liquid-cooled battery systems, most investigations have primarily focused on optimizing planar or serpentine flow patterns, micro-textured surfaces, or inlet-outlet configurations. However, the combined influence of channel number and channel height on thermal uniformity and flow distribution has not been comprehensively explored. Variations in channel height can substantially modify the local Reynolds number, pressure field, and heat transfer behavior, directly influencing coolant velocity and temperature gradients within the plate. Despite their clear importance, such geometric parameters are often simplified or assumed constant in existing models, leaving a gap in understanding how vertical channel geometry affects overall cooling performance.

Unlike most previous LCP studies, which compare different in-plane layouts at a fixed channel height, this study presents four plates that share the same footprint but differ only in the number of straight channels and their vertical height (2, 3, 4, and 5). This systematic variation allows us to isolate the role of vertical channel geometry in the trade-off between temperature uniformity and pressure drop in a realistic 60-cell cylindrical module. To address this research gap, the present study performs a comprehensive numerical analysis of multi-channel LCP configurations with different channel heights in a cylindrical LiB module. Four geometric layouts were designed under identical dimensional constraints to ensure a fair basis for comparison. Transient computational fluid dynamics simulations were carried out to examine the influence of channel geometry on coolant flow distribution, maximum temperature (T_{max}), and ΔT at three inlet velocities (0.1, 0.25, and 0.5 m/s). Both water and water-ethylene glycol (WEG) mixtures were used as working fluids to evaluate the effect of coolant type on thermal behavior. The novelty of this study lies in systematically quantifying how simultaneous variations in channel number and channel height affect both thermal uniformity and hydraulic behavior, which has not been addressed in previous LCP research.

2. MATERIAL AND METHOD

2.1. Geometry

LiBs are manufactured in various structural formats, including pouch, prismatic, and cylindrical types, each of which influences how heat is generated and dissipated during charge and discharge processes. Cylindrical cells are widely adopted in EV battery packs due to their mechanical robustness, uniform current distribution, and predictable radial heat conduction characteristics. In the present study, a cylindrical-cell battery module was modeled to analyze the impact of multi-channel LCP geometry on temperature uniformity and coolant flow distribution. The module consists of 60 individual cells arranged in a 6 × 10 grid (two parallel layers of 30 cells each), representing a typical mid-scale EV module configuration. Each cell has a diameter of 18 mm, a height of 65 mm, a nominal voltage of 3.6 V, and a capacity of 3.45 Ah. The thermophysical and electrochemical parameters used in the model are summarized in Table 1.

Table 1. Thermophysical and electrochemical properties of the cylindrical Li-ion battery cell used in the simulations

Property	Value
Positive (cathode) material	$LiFePO_4$
Negative (anode) material	Graphite
Battery diameter × height (mm)	18 x 65
Density (kg/m³)	2782
Specific heat (J/kg·K)	1087
Radial thermal conductivity (W/m·K)	1.2743
Axial thermal conductivity (W/m·K)	27.584
Heat generation rate at 4C (W/m³)	219,717.13
Nominal capacity (mAh)	3450
Nominal voltage (V)	3.6
Charge cut-off voltage (V)	4.2
Discharge cut-off voltage (V)	2
Maximum discharge current (A)	10

Each cell was modeled as a homogeneous, heat-generating solid with uniform volumetric heat generation corresponding to a 4C discharge rate. The 4C discharge rate was selected because it represents a realistic thermal load observed in electric vehicle battery modules during high-speed operation, peak power demand, rapid acceleration, and regenerative braking events. In order to suppress temperature escalation during operation and maintain uniform thermal conditions, multi-channel aluminum LCPs were integrated between the two layers of cylindrical cells to establish effective thermal coupling with the cell surfaces. Four geometric configurations were designed to systematically assess the influence of channel number and channel height on cooling performance. All designs maintain identical external dimensions for fair comparison, with channel height adjusted based on the number of channels, as follows:

(a) two-channel design (25 mm)
(b) three-channel design (15 mm)
(c) four-channel design (10 mm)
(d) five-channel design (8.5 mm)

A schematic representation of these LCP configurations is shown in Figure 1. Each plate is equipped with inlet and outlet manifolds to ensure uniform coolant distribution across the parallel channels, allowing consistent assessment of flow and temperature uniformity among the four designs.

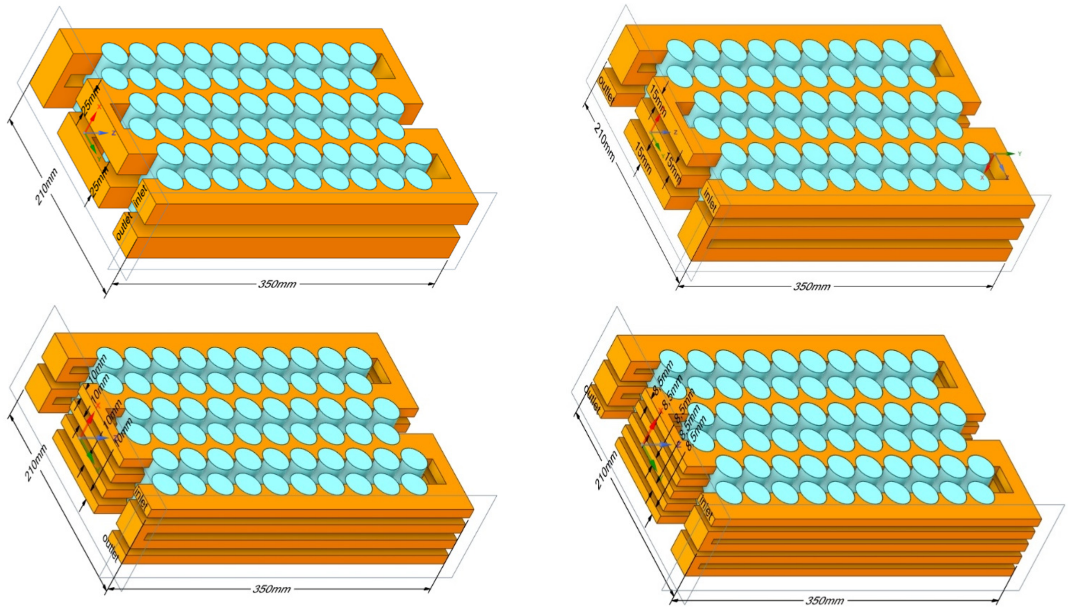

Figure 1. Schematic representation of the multi-channel LCP configurations used in this study: (a) two-channel (b) three-channel (c) four-channel, and (d) five-channel

The inlet and outlet manifolds are positioned on the same side of the plate to facilitate compact integration within the module assembly. During operation, the coolant enters through the inlet manifold, passes through the internal channels, and exits from the opposite outlet, forming a continuous flow path that enhances temperature uniformity across the module. The cooling plate material is aluminum, selected for its high thermal conductivity, low mass, and structural rigidity, which has made it a common choice in EV battery modules. The coolant domain was modeled using two working fluids: pure water and a 50:50 (v/v) mixture of water and ethylene glycol (WEG), both commonly used in electric vehicle applications due to their favorable heat-transfer characteristics and freeze protection capability. The thermophysical properties of the solid materials and coolant fluids at 298.15 K are summarized in Table 2. An inlet temperature of 298 K was selected because it corresponds to typical coolant supply temperatures in automotive battery thermal management systems and represents a realistic thermal boundary condition for EV operation.

Table 2. Thermophysical properties of materials and coolants used in this study

Material	Density (kg/m³)	Specific heat (J/kg·K)	Thermal conductivity (W/m·K)
Water (liquid)	998.2	4182	0.600
WEG	1040	3400	0.370
Aluminum block	2719	871	202.4

2.2. Governing Equations

Battery simulation approaches span multiple scales and levels of fidelity, ranging from simplified thermal networks to fully coupled electrochemical-thermal frameworks. At the module level, the multi-scale multi-domain (MSMD) concept provides a continuum description of charge and heat transport, resolving spatial variations of current density, potential, and temperature inside each cell [19].

Within this hierarchy, the Newman-Tiedemann-Gu-Kim (NTGK) model offers a semi-empirical representation of electrochemical heat generation by combining irreversible Joule losses with reversible entropic terms derived from experimental voltage-current characteristics [20]. The equivalent-circuit model (ECM) family, on the other hand, replaces detailed electrochemical kinetics with lumped R-C (resistor-capacitor) networks, coupling electrical and thermal behavior while maintaining low computational cost. Practically, real LiB cells exhibit anisotropic conductivity because of layered electrodes, separators, and the winding structure of jelly-roll assemblies. The through-plane conductivity is typically an order of magnitude lower than that in the in-plane direction, leading to directional heat spreading and possible hot-spot formation. Although such anisotropy can be explicitly modeled within MSMD or NTGK frameworks, its impact at the module scale is often dominated by boundary convection effects and coolant distribution.

To focus on the thermal performance of the LCP and to ensure computational tractability, the electrochemical domain was simplified. Each battery cell was represented as a homogeneous solid with uniform volumetric heat generation corresponding to the combined reversible and irreversible heat of a 4C discharge rate. This pragmatic approach, widely adopted in battery thermal management studies, preserves the overall heat-transfer characteristics while allowing systematic variation of geometric and flow parameters. All solid regions were assumed isotropic with effective thermal conductivity values, and radiation and contact resistances were neglected due to their minor contribution under forced-convection conditions. Temperature-dependent fluid properties were used for the coolant, while other materials were assumed constant at the reference temperature.

The flow field and heat transfer were described by the three-dimensional, transient, incompressible Navier-Stokes equations coupled with the energy equation. Conservation of mass, momentum, and energy can be expressed as follows [21-23] :

$$\frac{\partial \rho}{\partial t} + \nabla \cdot (\rho v) = 0 \quad (1)$$

$$\frac{\partial (\rho \mathrm{v})}{\partial t} + \nabla \cdot (\rho \mathrm{vv}) = -\nabla p + \nabla \cdot (\tau) + \rho \mathrm{g} \quad (2)$$

$$\frac{\partial (\rho \mathrm{E})}{\partial \mathrm{t}} + \nabla \cdot (\rho u \mathrm{E}) = -\nabla \cdot q + \nabla \cdot (\kappa \nabla T) + \Phi \quad (3)$$

Depending on the inlet velocity, the Reynolds number within the channels ranged from laminar to transitional and fully turbulent regimes. For Reynolds numbers above approximately 2300, the flow was treated as turbulent using the standard k-ε model, which solves additional transport equations for the turbulence kinetic energy (k) and its dissipation rate (ε) [24]:

$$\frac{\partial (\rho k)}{\partial \mathrm{t}} + \nabla \cdot (\rho u k) = \nabla \cdot \left(\frac{\mu_t}{\sigma_k} \nabla k\right) + P_k - \epsilon \quad (4)$$

$$\frac{\partial (\rho \epsilon)}{\partial t} + \nabla \cdot (\rho u \epsilon) = \nabla \cdot \left(\frac{\mu_t}{\sigma_k} \nabla \epsilon\right) + C_{1\epsilon} \frac{\epsilon}{k} P_k - C_{2\epsilon} \epsilon \quad (5)$$

Radiative heat transfer and interfacial thermal contact resistances were neglected, as their contribution was found to be negligible compared with conduction and forced convection. Heat transfer within the solid domains follows Fourier's law, whereas convective heat exchange between the battery surface and the coolant flow conforms to Newton's law of cooling. Accordingly, the transient heat conduction equation can be expressed as:

$$\rho C_p \frac{\partial T}{\partial t} + \nabla \cdot (\rho C_p u T) = \nabla \cdot (k \nabla T) + q^m \quad (6)$$

where ρ denotes density (kg/m^{-3}), C_p the specific heat capacity (J kg^{-1} K^{-1}), T the temperature (K), u the velocity vector (m s^{-1}), k the thermal conductivity (W m^{-1} K^{-1}). The term q^m represents the volumetric heat generation rate in the battery cell due to electrochemical reactions and internal resistance during discharge.

2.3. Numerical Implementation and Grid Verification

The computational domain was discretized using an unstructured hybrid mesh to accurately resolve the coupled fluid and solid regions of the battery module. The mesh was predominantly composed of hexahedral elements in the main flow passages and tetrahedral elements in regions of geometric curvature. Local grid refinement was applied along the channel walls and at the cell-plate contact interfaces to ensure precise resolution of boundary layer development and conjugate heat-transfer behavior. This meshing strategy provided a balanced compromise between numerical accuracy and computational efficiency, enabling stable and physically consistent solutions throughout the simulation domain.

The simulations were conducted in transient mode, allowing the temperature and velocity fields to evolve dynamically until reaching a quasi-steady state. A time-step independence test was performed using Δt = 0.1s, 0.5s, 1s, and 2s under identical boundary conditions corresponding to a 4C discharge rate and a coolant inlet velocity of 0.25 m/s. The variation in T_{max} between the 1s and 0.1s time steps was below 0.4 %, confirming temporal convergence. Accordingly, a time-step size of 1s was adopted for all subsequent simulations as an optimal balance between computational cost and numerical accuracy. The final computational domain and mesh structure are illustrated in Figure 2, where the dense refinement around the cylindrical cell surfaces and coolant channels indicates the regions of dominant thermal gradients and conjugate heat transfer.

A mesh independence study was carried out using grids of approximately 0.5×10^6, 1×10^6, 2×10^6, 3×10^6, and 4×10^6 cells. The differences in Tmax, ΔT, and pressure drop between the 1×10^6-cell mesh and the finer grids were below 1%, showing that further refinement did not improve the results. Therefore, a grid of about 1×10^6 cells was used for all simulations. Near-wall inflation ensured adequate boundary-layer resolution, giving an overall y^+ range of 20-60, which is suitable for the standard k–ε turbulence model.

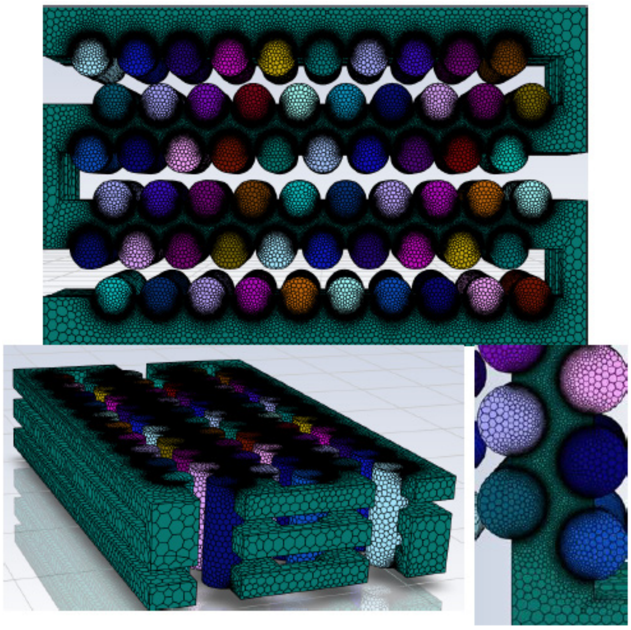

Figure 2. Computational domain

2.4. Numerical Simulation and Validation

The thermal behavior of LiBs originates from several coupled electrochemical processes, including irreversible Joule heating, entropic heat during lithium intercalation and deintercalation, and additional side reactions at the electrode-electrolyte interface. The net heat generation depends on the state of charge, discharge rate, and internal resistance, all of which influence the local temperature distribution inside the cell. To maintain computational efficiency and focus on thermal management performance, these combined effects were represented by an equivalent volumetric heat generation rate corresponding to a 4C discharge condition, incorporating both reversible and irreversible contributions under high-power operation.

For the present study, each cell was modeled as a uniform heat-generating solid in the battery module, and the surrounding fluid domain represented the LCP structure. Transient simulations were conducted over 700s, allowing the T_{max} to evolve until thermal equilibrium was reached. The initial temperature of all domains and the coolant inlet were set to 298.15 K. In the validation stage, the same heat-generation model was applied under no-cooling conditions (adiabatic surroundings) to replicate the reference case reported by Zhang et al. [25].

The comparison between the reference study and the present numerical model is presented in Figure 3. Both curves exhibit a nearly linear rise in T_{max} with time, confirming that the implemented thermal source term accurately reproduces the expected heat generation behavior during high-rate discharge. The maximum deviation between the predicted and reference temperatures remained within 1.2% throughout the 700s period, validating the numerical accuracy of the simplified model. This validation confirms that the present simulation framework can reliably predict transient thermal responses of cylindrical lithium-ion cells under intensive discharge conditions. The verified model was subsequently used to assess the thermal performance of the multi-channel LCP configurations introduced in Section 2.1.

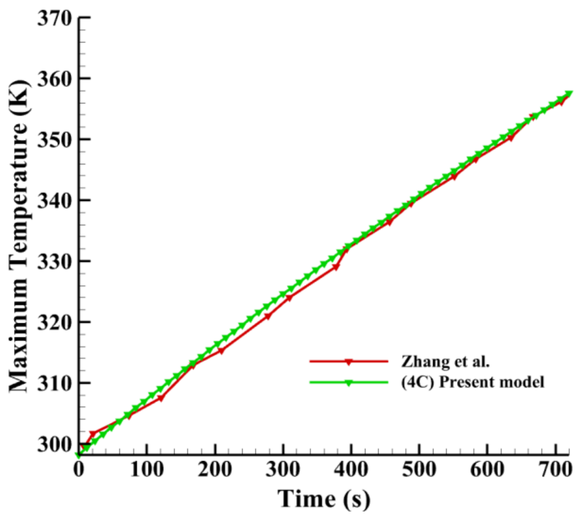

Figure 3. Validation of the simulated model [25]

After model validation, the simulation matrix presented in Figure 4 was designed to explore the influence of geometric and operational parameters on the thermal behavior of the module. The analysis considered four LCP configurations, two coolant formulations, and three inlet velocities (0.1, 0.25, and 0.5 m/s) under a constant 4C discharge rate. These combinations provided a systematic framework for evaluating both temperature uniformity and overall cooling effectiveness across all cases.

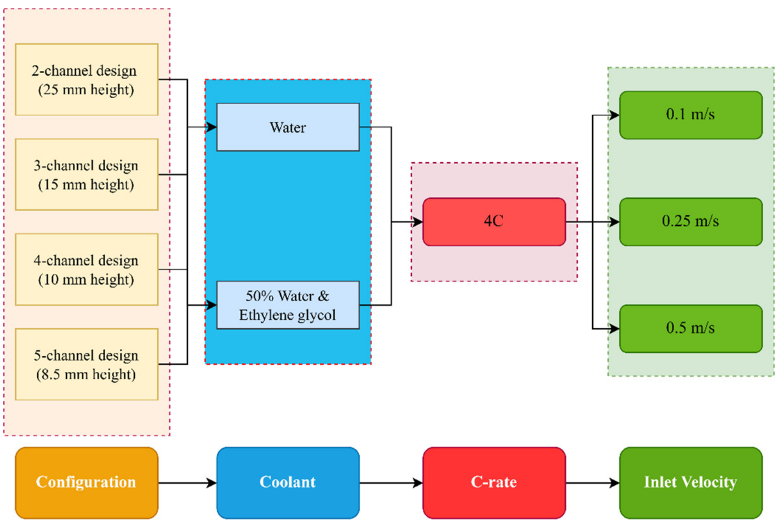

Figure 4. Roadmap of the study

3. RESULTS AND DISCUSSION

Figure 5 shows the steady-state temperature contours for the four LCP configurations at a coolant velocity of 0.1 m/s, using either water or WEG as the working fluid. The two-channel plate demonstrates superior temperature uniformity and the lowest cell temperatures under cooling with water. Decreasing the channel height in the designs with three, four, and five channels weakens local convection and reduces flow mixing between adjacent passages.

In the case of the WEG (Figure 5b), the temperature increases by approximately 1 to 2 K under the same operating conditions. This rise results from the mixture's lower thermal conductivity and higher viscosity, which weaken heat transfer and slow the renewal of the boundary layer along the cell surfaces. The temperature field appears slightly more layered, especially in the configurations with four and five channels, where higher flow resistance leads to reduced circulation. At this low inlet velocity, the two-channel design achieves the best cooling performance by maintaining both a low T_{max} and a uniform temperature distribution. Increasing the number of channels extends the flow coverage but also causes higher pressure losses and lower convective efficiency because of the smaller flow area and limited coolant mixing.

The differences observed between channel designs are closely linked to how the coolant distributes and moves within the plate. In the two-channel configuration, the greater channel height reduces hydraulic resistance and promotes a more uniform velocity field, allowing the coolant to sweep the cell surfaces efficiently and maintain strong convective heat transfer. When additional channels are added, the reduced channel height restricts the available flow area and forces the coolant into narrower paths, increasing resistance and reducing through-flow. This leads to lower velocities and small recirculation regions, particularly near the manifold connections and side walls, where heat removal becomes less effective. These flow characteristics become more pronounced in the four- and five-channel configurations, resulting in higher Tmax and reduced temperature uniformity.

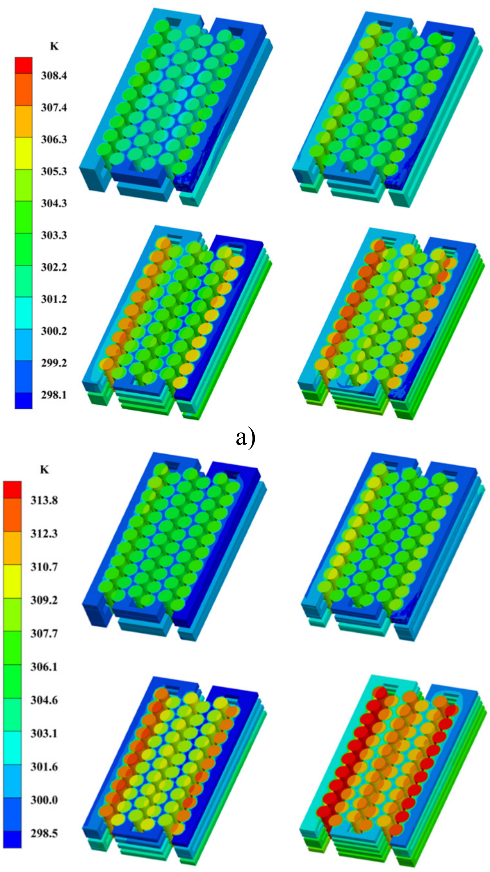

Figure 5. Temperature contours of the battery module at 0.1 m/s coolant velocity for different working fluids: (a) water and (b) WEG

As shown in Figures 6a-c, the temperature evolution of the battery module follows a clear transition from transient to steady state. During the initial 100 s, the temperature increases rapidly as internal heat generation dominates, and then gradually approaches a steady state once heat removal by the coolant becomes sufficient. At the lowest inlet velocity of 0.1 m/s, limited convection emphasizes the geometric differences among the four LCP configurations. The two-channel design maintains the lowest temperature, around 305 K, whereas the five-channel configuration reaches nearly 308 K, primarily because reduced flow mixing and the smaller channel height restrict local heat transfer.

The convective heat transfer improves for all configurations at an inlet velocity of 0.25 m/s, leading to a temperature drop of around 3 K. The two-channel plate continues to demonstrate the most effective thermal performance by providing a stable and uniform temperature field. Only a slight additional cooling of less than 0.5 K is observed as the velocity is further increased to 0.5 m/s (Figure 6c), which suggests that the flow has entered an efficient convective regime where higher velocities bring little additional benefit. These results indicate that the most significant increase in heat dissipation occurs in the low-to-medium coolant speed range. Beyond this range, the decrease in T_{max} becomes insignificant. This observation is consistent with previous numerical and experimental studies on liquid-cooled battery systems, which have reported that most convective enhancement occurs before the flow is fully developed. In addition, the thermal trends also correspond to the relative pressure drop of the channel designs, as configurations with higher hydraulic resistance require greater pumping power while still providing weaker temperature reduction.

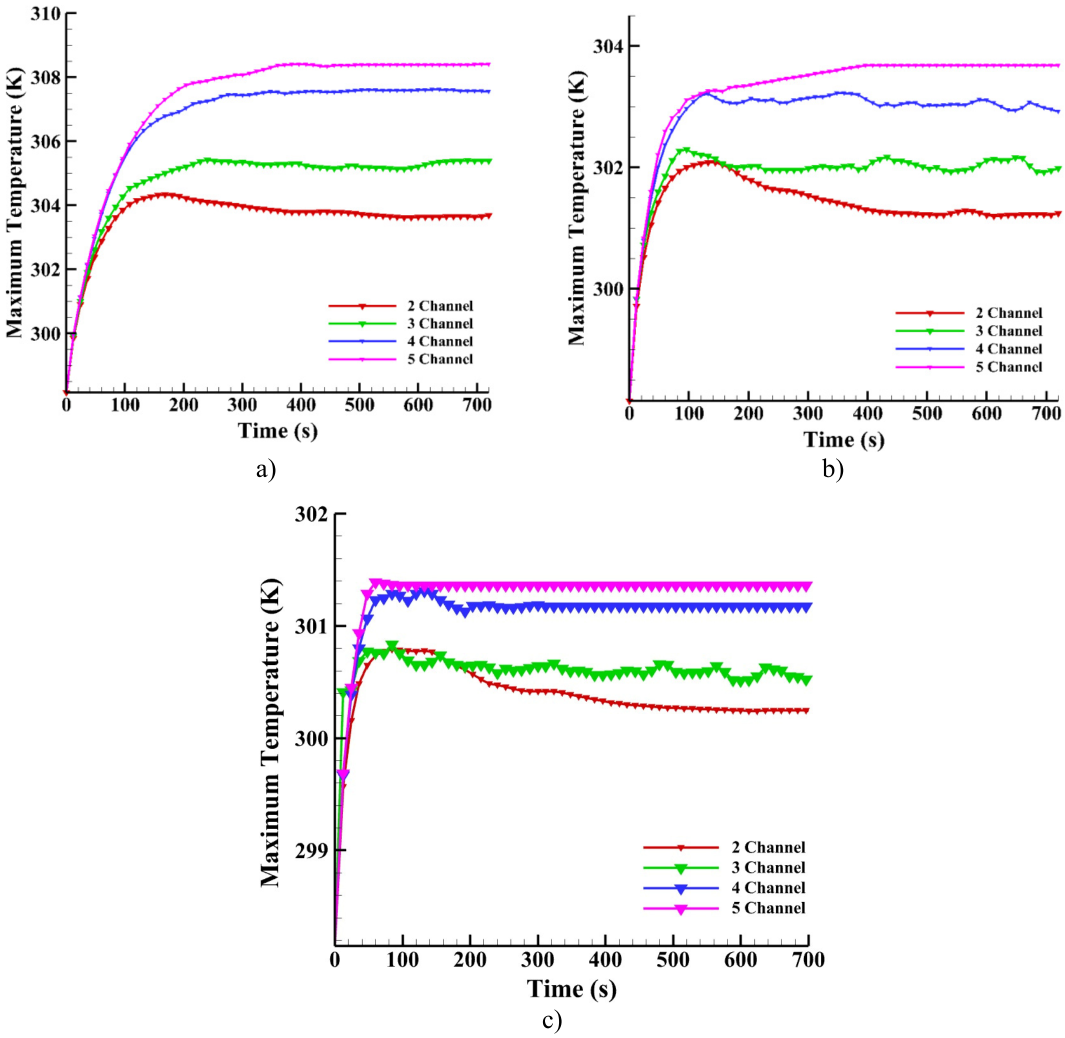

Figure 6. Evolution of the T_{max} for the four LCP configurations at different coolant velocities using water as the working fluid: (a) 0.1 m/s, (b) 0.25 m/s, and (c) 0.5 m/s

The overall temperature field exhibited a similar pattern to that of pure water after the coolant was replaced with the WEG, as shown in Figures 7a-c. The temperature levels increased up to 2 K in all tested velocities, mainly due to the lower thermal conductivity and higher viscosity of the mixture, which reduce the Reynolds number and weaken convective heat transfer. Despite this temperature rise, the relative thermal ranking of the LCP geometries remained unchanged. The two-channel configuration achieved the lowest T_{max}, whereas the four- and five-channel plates exhibited higher steady-state values because their smaller hydraulic diameters restricted coolant mixing and increased hydraulic resistance. These results confirm that decreasing channel height limits both heat removal and temperature uniformity, whereas the two-channel plate provides the most effective balance between cooling capacity and flow resistance, keeping T_{max} below 306 K and ΔT within 3 K under nominal operating conditions.

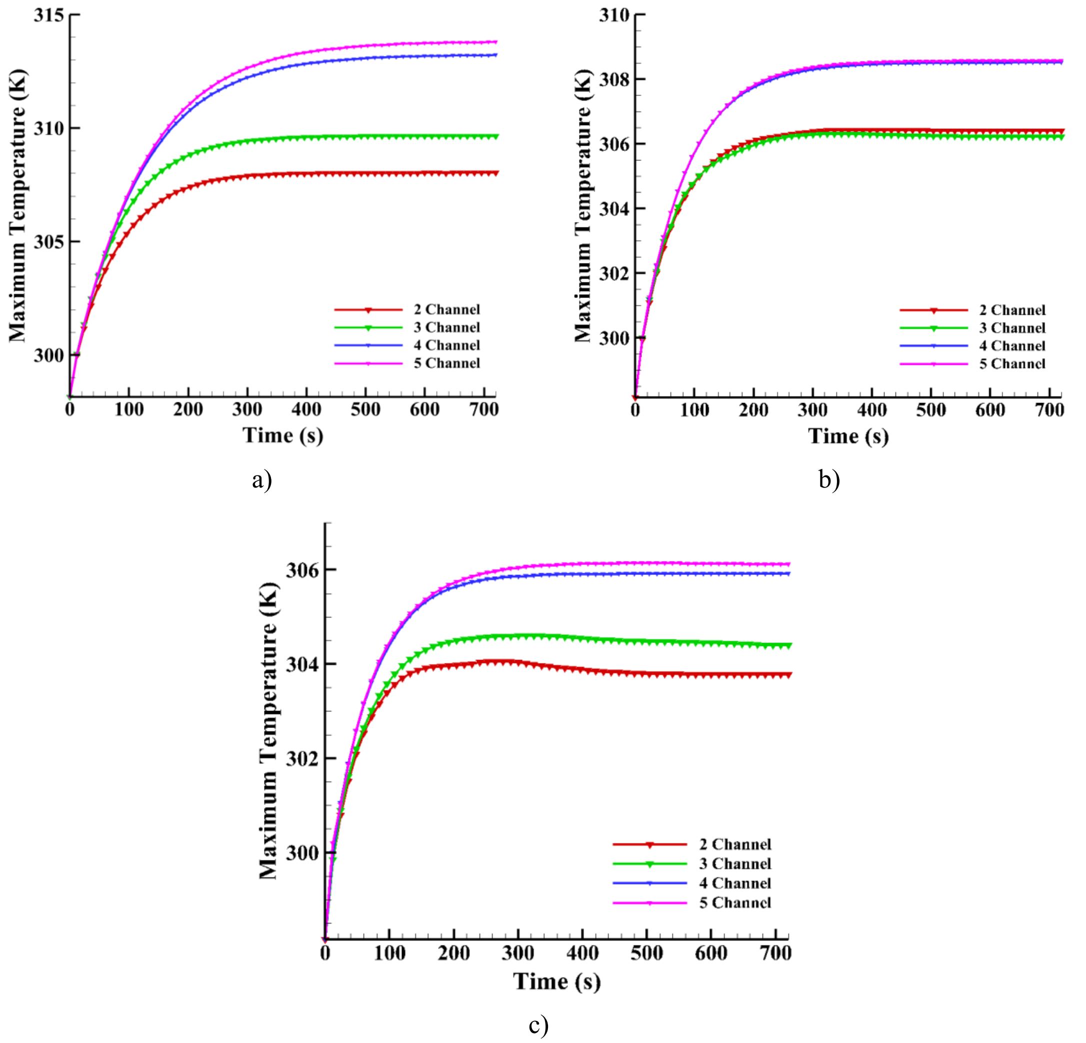

Figure 7. Evolution of the T_{max} for the four LCP configurations at different coolant velocities using the WEG as the working fluid: (a) 0.1 m/s, (b) 0.25 m/s, and (c) 0.5 m/s

Figure 8 illustrates the maximum ΔT among the battery cells for different channel configurations and coolant velocities. In both coolant types, ΔT decreases markedly with increasing inlet velocity, confirming that stronger convection enhances temperature uniformity. For the water-cooled cases, ΔT ranges from about 4 to 5 K at 0.1 m/s to below 3 K at 0.5 m/s, while the WEG exhibits slightly higher temperature variations due to its reduced thermal conductivity. At all velocities, the two-channel configuration achieves the smallest ΔT, maintaining uniform temperature distribution along the coolant path. In contrast, four- and five-channel designs show larger temperature gradients, especially at low flow rates, attributed to weaker cross-channel mixing and increased thermal resistance. These results emphasize that channel height and flow rate jointly control thermal uniformity: decreasing the channel height to fit more channels offers broader surface coverage but limits the convective balance, leading to localized hot zones. Consequently, the two-channel plate again emerges as the most thermally uniform configuration under all tested conditions.

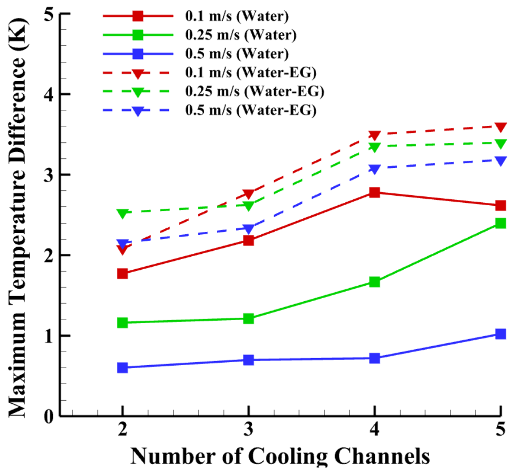

Figure 8. Variation of maximum ΔT between battery cells for different channel configurations and coolant velocities using water and the WEG

The combined temperature and ΔT analyses offer a comprehensive understanding of how geometry and coolant type influence the overall heat dissipation process. While the thermal contours highlight the temperature distribution on the battery surfaces, it is equally important to examine the internal coolant flow behavior within the LCP. Understanding the internal flow structure helps explain the observed differences in temperature uniformity and local hot-spot formation.

Figure 9 illustrates the velocity contours inside the LCPs, which demonstrate how the number of channels affects flow distribution and mixing. In the two-channel design, the coolant flows uniformly through each channel, maintaining a nearly symmetric velocity field with minimal recirculation zones. This promotes effective contact with the cell surfaces and directly contributes to its enhanced thermal performance. The three-channel configuration maintains a balanced flow field but begins to show mild velocity decay near the middle section as the flow divides into smaller branches. In contrast, the four- and five-channel plates exhibit noticeable velocity stratification and localized low-speed regions, particularly near the outlet manifold. As the channel height decreases, the hydraulic diameter and Reynolds number are reduced, leading to weaker convection and more pronounced boundary-layer overlap along the inner walls. Small stagnation pockets appear in corner regions where coolant recirculation occurs, reducing overall heat-transfer effectiveness.

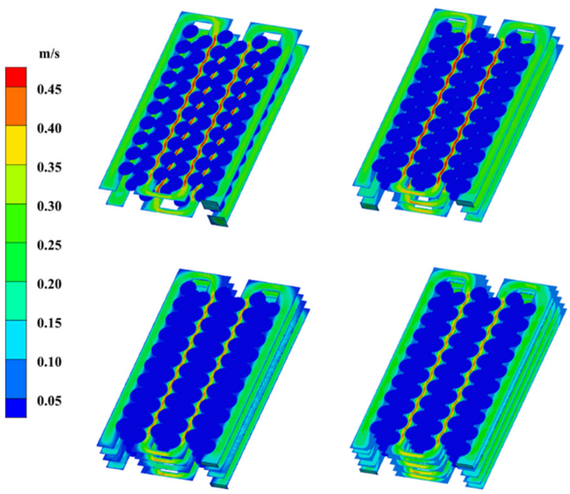

Figure 9. Velocity contours of coolant flow for different channel configurations at an inlet velocity of 0.25 m/s (water)

4. CONCLUSIONS

This study numerically investigated the thermal behavior of multi-channel LCPs for cylindrical LiB modules under various geometric and operating conditions. The results demonstrated that both channel height and flow rate play key roles in controlling heat removal, temperature uniformity, and coolant distribution. Among the analyzed configurations, the two-channel LCP consistently provided the lowest T_{max} and the most uniform thermal field for all coolant types and velocities. Its larger hydraulic diameter and simpler flow path led to higher convective efficiency and minimal pressure loss. In contrast, increasing the number of channels led to thinner flow passages and stronger viscous effects, causing localized hot spots and non-uniform velocity profiles, particularly near the outlet manifold.

The coolant velocity strongly affected heat transfer at low flow rates but showed diminishing returns at higher velocities. Increasing the flow rate from 0.1 to 0.25 m/s significantly improved heat transfer and reduced ΔT by up to 40%, whereas a further increase to 0.5 m/s yielded only marginal thermal benefit (<1 K) while noticeably raising pumping power. The WEG resulted in slightly higher temperatures (by about 1 to 2 K) than pure water, due to its lower thermal conductivity and higher viscosity, though the overall performance trends remained similar. Velocity contour analysis confirmed that the main cause of temperature non-uniformity in narrow channels is the disturbance in flow distribution. The two-channel plate maintained a stable flow field without major recirculation, aligning with its superior thermal results.

In practical terms, these findings highlight that a moderate coolant velocity (≈0.25 m/s) combined with a two-channel LCP design offers the optimal balance between thermal performance, flow uniformity, and energy efficiency. The results contribute to the design of lightweight and scalable cooling systems suitable for compact EV battery modules. Future work will focus on extending this approach to curved and multi-inlet channel designs, as well as incorporating conjugate electrochemical-thermal coupling to further enhance model accuracy.

5. REFERENCES

1. Tosun, E., Keyinci, S., Yakaryılmaz, A.C., Yıldızhan, Ş. & Özcanlı, M. (2024). Evaluation of lithium-ion batteries in electric vehicles. *International Journal of Automotive Science and Technology, 8*(3), 332-340.
2. Zaino, R., Ahmed, V., Alhammadi, A.M. & Alghoush, M. (2024). Electric vehicle adoption: A comprehensive systematic review of technological, environmental, organizational and policy impacts. *World Electric Vehicle Journal, 15*(8), 1-47.
3. Erdoğan, B., Tan, A. & Tümay, M. (2024). Genetic algorithm enhanced resonant converter design for battery charging applications in electric vehicles. *Cukurova University Journal of the Faculty of Engineering, 39*(4), 1129-1142.
4. International Energy Agency (IEA), (2023). *Global EV Outlook 2023.*
5. Uzun, M. (2025). Thermal and electrical analysis of 26650 li-ion batteries in series connection using the NTGK model and virtual simulations. *European Mechanical Science*, *9*(1), 46-58.
6. Tosun, E., Keyinci, S., Yakaryilmaz, A.C. & Ozcanli, M., (2025). A study on the removal of heat generated by a lithium-ion battery module: A fan-assisted battery cooling approach. *Processes,13*(3), 848.
7. Marri, G.K., Ee, Y.J., He, Z. & Ho, J.Y. (2026). Recent advancements in internal and external thermoregulation strategies for lithium-ion batteries. *Renewable and Sustainable Energy Reviews, 225*, 116127.
8. Keyinci, S., Ilinčić, P., Tosun, E., Uzun, M., Yakaryilmaz, A.C. & Ozcanli, M. (2025). Design and performance analysis of a curved channel liquid cooling system for battery thermal management. *Thermal Science and Engineering Progress, 63*, 1-19.
9. Yakaryilmaz, A.C., Bicak, M.I., Tosun, E., Keyinci, S. & Ozcanli, M. (2025). Experimental assessment of battery thermal management in a lithium-ion battery module under varying ambient temperatures and fan-assisted air-cooling strategies. *Thermal Science and Engineering Progress, 65*, 103900.
10. Akkuş, F. & Işik, M.Z. (2025). Investigation of thermal performance of pipe-supported air-cooled systems in lithium-ion battery packs. *Cukurova University Journal of the Faculty of Engineering, 40*(4), 855866.
11. Singh Rawat, S. & Kumar, R. (2025). Battery thermal management systems for electric vehicles: current trends and strategies for sustainable transportation. *Engineering Research Express, 7*(3), 1-22.

12. Luo, J., Xia, W., Wang, S., Li, D. L. & Kang, X. (2025). Comprehensive application of phase change materials in lithium-ion battery thermal management: From single cooling to coupled systems. *Energy Technology, 13*, 2401930.
13. Li, P., Zhao, J., Zhou, S., Duan, J., Li, X., Zhang, H. & Yuani J. (2023). Design and optimization of a liquid cooling thermal management system with flow distributors and spiral channel cooling plates for lithium-ion batteries. *Energies, 16*(5), 2196.
14. Li, L., Mao, Z., Cai, T., Hu, X. & Xu, J. (2025). Thermal–hydraulic performance optimization of Tesla-type minichannel structures for AUV battery thermal management using genetic algorithms. *Thermal Science and Engineering Progress, 67*, 104130.
15. Lai, Y., Ding, J. & Liu, L. (2025). Numerical investigation on the cooling performance of lithium-ion battery using liquid cooled-plate with integrated grooves and secondary microchannel structures. *International Journal of Thermal Sciences, 217*, 110094.
16. Akbarzadeh, M., Kalogiannis, T., Jaguemont, J., Jin, L., Behi, H., Karimi, D., Beheshti, S.H., Mierlo, J.V. & Berecibar, M. (2021). A comparative study between air cooling and liquid cooling thermal management systems for a high-energy lithium-ion battery module. *Applied Thermal Engineering, 198*, 117503.
17. Dubey, D., Mishra, A., Shriyan, H.C., Pratap, T. & Pandey, R. (2024). Improved thermal management of lithium-ion battery module through microtexturing of serpentine cooling channels. *Energy Technology, 12*(5), 2301253.
18. Monika, K., Punnoose, E.M. & Datta, S.P. (2024). Multi-objective optimization of cooling plate with hexagonal channel design for thermal management of Li-ion battery module. *Applied Energy, 368*, 123423.
19. Schmidt, A., Oehler, D., Weber, A., Wetzel, T. & Ivers-Tiffée, E. (2021). A multi scale multi domain model for large format lithium-ion batteries. *Electrochimica Acta, 393*, 139046.
20. Zhu, H., Ma, Y., E, J. & Wei, S. (2024). Channel structure design and optimization for immersion cooling system of lithium-ion batteries. *Journal of Energy Storage, 77*, 109930.
21. Fan, L., Li, J., Chen, Y., Zhou, D., Jiang, Z. & Sun, J. (2024). Study on the cooling performance of a new secondary flow serpentine liquid cooling plate used for lithium battery thermal management. *International Journal of Heat and Mass Transfer, 218*, 124711.
22. He, P., Lu, H., Fan, Y., Ruan, H., Wang, C. & Zhu, Y. (2023). Numerical investigation on a lithium-ion battery thermal management system utilizing a double-layered I-shaped channel liquid cooling plate exchanger. *International Journal of Thermal Sciences, 187*, 108200.
23. Qian, Z., Li, Y. & Rao, Z. (2016). Thermal performance of lithium-ion battery thermal management system by using mini-channel cooling. *Energy Conversion and Management, 126*, 622-631.
24. Bao, Y. & Wang, H. (2022). Numerical study on flow and heat transfer characteristics of a novel Tesla valve with improved evaluation method. *International Journal of Heat and Mass Transfer, 187*, 122540.
25. Zhang, B., Zeng, Z., Yuan, N. & Shi, H. (2025). Numerical investigation of lithium-ion battery thermal management system performance influenced by physical properties of PCM. *Journal of Energy Storage, 117*, 116141.